

EUROPEAN ORGANIZATION FOR NUCLEAR RESEARCH

MRH/LR/HHU/afm

CERN/PS/85-56 (AA)

COMBINED QUADRUPOLE-SEXTUPOLE MAGNETS  
FOR THE CERN ANTIPROTON COLLECTOR

M.R. Harold  
Rutherford Appleton Laboratorz, Didcot, England

L. Rinolfi and H.-H. Umstätter  
CERN, Geneva, Switzerland

(Paper presented at the 9th International Conference  
on Magnet Technology (MT-9), Zürich, 9-13 September 1985)

Geneva, Switzerland  
September 1985

COMBINED QUADRUPOLE-SEXTUPOLE MAGNETS FOR THE CERN ANTIPROTON COLLECTOR

M R Harold\*, L Riolfi\*\*, H H Umstatter\*\*

\* Rutherford Appleton Laboratory, UK. \*\* CERN, Geneva, Switzerland.

Abstract - The CERN antiproton source is being upgraded by the addition of a new large acceptance storage ring: the antiproton collector (AC), which is situated around the existing accumulator (AA). The arcs of the AC contain combined quadrupole-sextupole magnets. The pole contours are defined by one root of a polynomial whose coefficients are adjusted such that the integral of the field gradient has the required linear gradient across the aperture. The field integrals are obtained from the 3D computer code TOSCA. In order to achieve an ultimate field gradient quality of 1 part in 1000, provision has been made for shimming the pole ends. The results of the magnetic measurements are presented and compared with the computed predictions.

INTRODUCTION

In 1983 approval was given for the construction at CERN of the antiproton collector, an essential component in the scheme [1] to increase the accumulation rate of antiprotons by at least an order of magnitude. The AC is a storage ring concentric with the existing AA, but having a slightly larger circumference (see Fig. 1) and a considerably increased acceptance (200  $\mu$ m.mrad). Every 2.4 sec 3.5 GeV/c antiprotons from an improved target station will be injected into the AC, where they will be pre-cooled both in momentum and betatron phase space before being ejected and transferred to the AA.

The AC lattice is of the separated function type, and in order to satisfy the many restraints governing the design, the 56 quadrupoles are divided into seven families. Two of the quadrupoles (type QS) are special in order to facilitate injection and extraction, and will be reported on elsewhere. The narrow quadrupoles (QN) comprise three families, two of which contribute to the bending of the stored beam and so are, in fact, combined function magnets. The wide quadrupoles (QW) are combined quadrupole-sextupoles whose function is to both focus the stored beam and to correct the chromaticity introduced by the bending magnets. There are four families within the QW-type - the QFW has a sextupole component  $s = 0.6/m$  where

$$s = \int B'' ds / \int B' ds,$$

and the QDW has  $s = 1.42/m$  and operates at three different gradient levels. Table 1 gives a summary of the quadrupole parameters. It should be noted that the sextupole terms are considerably larger than those used in the wide quadrupoles of the AA [2], where  $s = 0.14/m$ .

It is required that for each quadrupole the variation of gradient integral ( $\Delta G/G$ ), the effective length ( $L_{eff}$ ), and the gradient integral (G) should all meet the tolerance of 1 part in 1000. Since all the

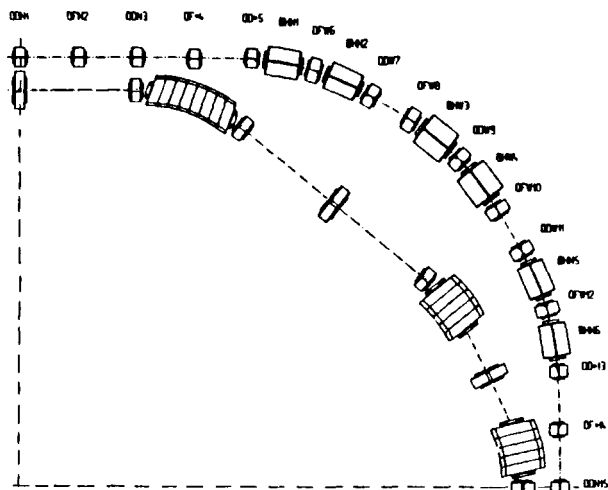


Fig 1 - A quadrant of the AC, surrounding the AA.

TABLE 1

QN Type			
Name	QDN3	QFN4	QDN5
Inscr. radius (mm)	110	110	110
Turns per pole	19	17	15
Current (A)	1851	1851	1851
Bending angle (mrad)	-	30	18
g (T/m)	6.811	6.248	5.669
G (T)	4.849	4.567	4.188

QW Type				
Name	QFW6	QDW7	QFW8	QDW9
Inscr. radius (mm)	132	132	132	132
Turns per pole	20	22	26	17
Current (A) (est)	(1830)	(1890)	1782	(1899)
g (T/m)	5.256	5.926	6.504	4.640
G (T)	3.983	4.468	4.884	3.350
s (/m)	1.425	1.425	0.600	1.425

quadrupoles are connected in series electrically, this is achieved in the case of the QN's by having different numbers of turns per pole for each family, and by small adjustments to the pole-lengths using detachable end-shims. For the QW's, trim power supplies provide another necessary variable. Additionally, all the quadrupoles are provided with the facility for adding washers to the pole ends for small, localised, length variations [2].

DESIGN

It was decided from the outset that no prototypes were to be built, and that all the magnets' dimensions were to be defined by the use of the three-dimensional magnetostatics program TOSCA [3]. In this manner significant savings in money and manpower would be possible.

The Narrow Quadrupole

The design philosophy adopted was similar to that used for the AA quadrupoles [2], and is briefly recalled here. The pole profile, including shims, was first optimised for a pure quadrupole field using a two-dimensional (2D) program such as MAGNET [4] or PE2D [5]. TOSCA was then run, with the same profile, in a pseudo-2D mode where the iron boundary conditions and the coils are defined so as to make the magnet infinitely long in the beam direction. The TOSCA mesh was then adjusted until the results were in close agreement (1 or 2 parts in 1000 in  $\Delta g/g$ , where  $g = dB/dx$  at the longitudinal centre of the magnet), the MAGNET/PE2D results being obtained with finer meshes. Because of the symmetry of the QN, it was only necessary to describe 45°-worth of the magnet cross-section, and this allowed the use of a high proportion of quadratic elements in the vital areas (pole-tip and air-gap) whilst maintaining reasonable run-times (about 1 hour on an IBM). The mesh is shown in Fig. 2, with the quadratic elements shaded.

The full 3D model was introduced, and after adjustments to correct the effective length, the field integrals were analysed as a function of lateral displacement (x-axis) to extract the 12-pole component created by the coil- and pole-ends. This was then reversed in sign, multiplied by the ratio of  $L_{eff}$  to iron length (0.72/0.6) and included in a new pole profile by the following method [2], [6]. The complex potential  $w = u+iv$  is expanded in a truncated power series (i.e. a polynomial) in  $z = x+iy$  up to the 12-pole term. Putting  $v = \text{const.}$  for an equipotential line one can write the complex polynomial equation

$$w(z) - (u + i \cdot \text{const}) = 0$$

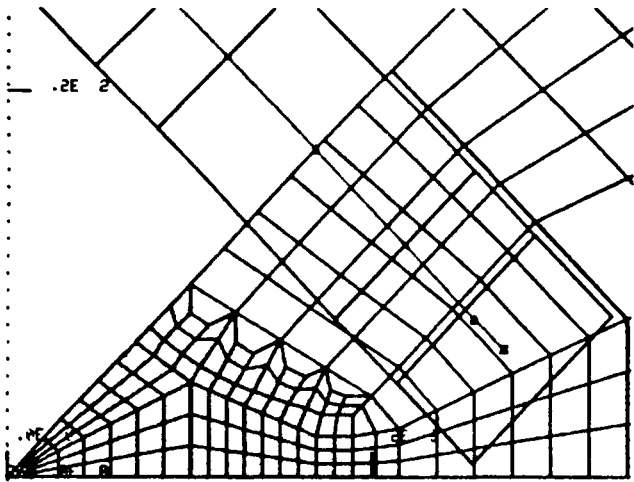


Fig 2 - QN. Part of the TOSCA mesh.

which is solved numerically for  $z = x+iy$ . As  $u$  varies these roots yield all points  $(x, y)$  along the equipotential which is the new pole profile. Finally the shims were adjusted in height to optimise the field pattern, using a 2D program to obtain a guide on the effectiveness of the shims.

All this was done for a magnet excitation in the middle of the expected operational range. When the QN was run at the highest current, it was noted that TOSCA predicted 8% iron loss and a fall-off in field quality at large radii. Fortunately the good field region required for those quadrupoles operating at this level is very small. The predictions and measurements of the QN are discussed later.

Wide Quadrupoles

For the QW's, the same procedure was followed (see Fig. 3 for the mesh). Due to the fact that these

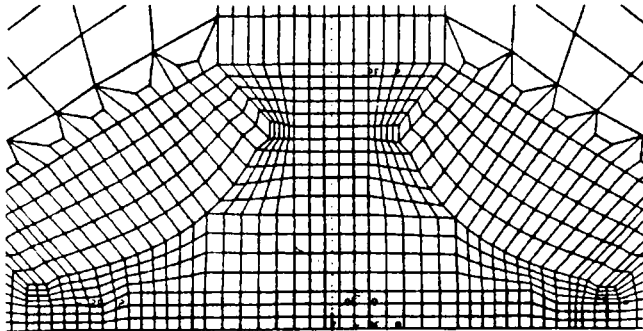


Fig 3 - QW. Part of the TOSCA mesh.

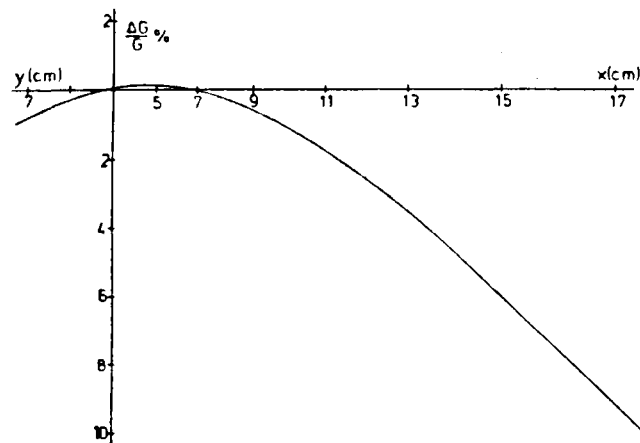


Fig 4 - QFW. G vs x. No end-effect correction.

quadrupoles are not symmetric about the 45° line, an 8-pole component was present in 3D as well as the 12-pole. This is illustrated in Fig. 4, where  $\Delta G/G$  is plotted against  $y$  (vertical) on the left and  $x$  on the right of zero, using a quadratic scale for the abscissa. In this system of coordinates the 8- and 12-pole can be recognised by inspection: the 8-pole shows up as a slope at  $x = y = 0$  and the 12-pole as a parabola.

When the 8- and 12-poles had been corrected in the profile, and the gradient error seen to be small in the central region, the required sextupole component (again increased by  $L_{eff}/L_{iron}$ , 0.75/0.62), was put into the profiles. It was not possible to obtain quite such good agreement in 2D between PE2D and TOSCA. The TOSCA mesh was slightly coarser than that for the QN, and there were proportionally far fewer quadratic elements because of the need to describe 180° of the quadrupole when the sextupole term was introduced. Although it was possible to increase the number of nodes by a factor of two, if this had been done the turn-round time of the job would have been impossibly long.

Some adjustments were made to the shim heights, but lack of time prevented a full optimisation. In the case of the QFW, because of the asymmetry introduced by the sextupole component the shims on the positive  $x$  side were very much more saturated than those on the negative  $x$  side, and allowance had to be made for this. For the QDW, the poles were made narrower to take advantage of the smaller good-field region required, and the asymmetry did not cause such a problem. However, QDW has to operate at three field levels, and the integrated sextupole component was predicted by TOSCA to vary significantly over the range (Fig. 5), and so a small adjustment to the sextupole term was made in order to make the value correct in the middle of the range.

RESULTS AND DISCUSSION

QN

Figures 6 and 7 show the predictions and the results of measurements made at CERN on the first production QN. This quadrupole has 19 turns/pole, and

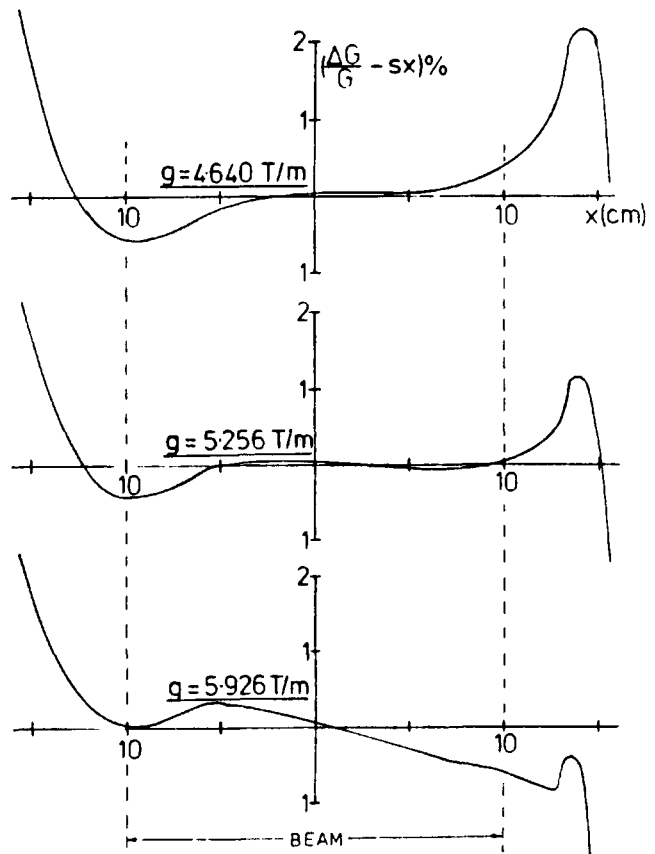


Fig 5 - QDW. G vs x at three gradient levels. Note that the required sextupole strength has been subtracted from the ordinates.

the current was reduced in order to simulate the 17 and 15 turns/pole types. The excellent results for this magnet were confirmed later on the second QN, which was of the 17-turn type. The measurements were performed with the same apparatus used for the AA quadrupoles [7]. A long coil-pair is moved across the magnet aperture and the induced volts integrated using an HP2401C integrator. The coil is then transferred to the magnet centre and rotated about its axis to measure G. A short (10 cm) coil-pair was used to measure gradients at the longitudinal centre of the quadrupole.

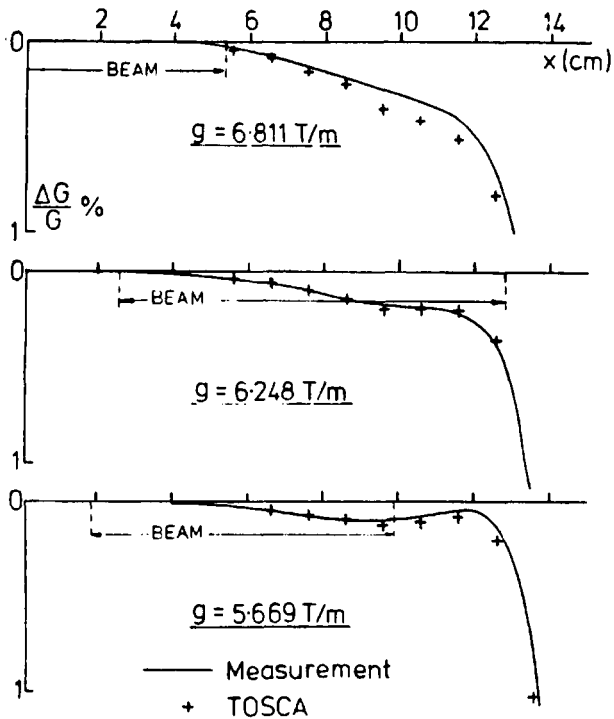


Fig 6 - QN. G vs x at three gradient levels. Prediction and measurement.

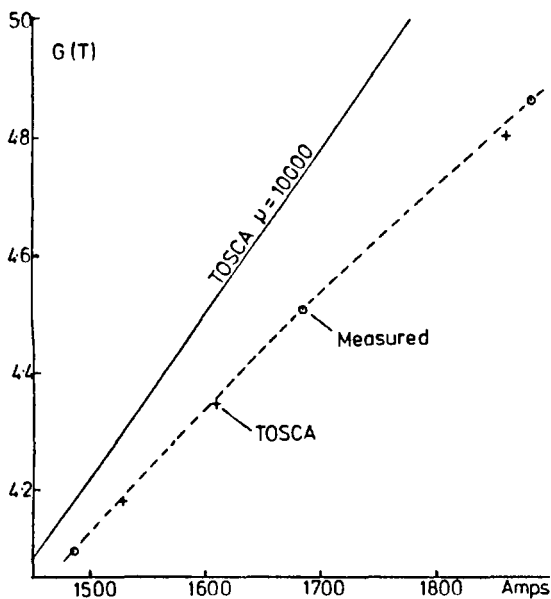


Fig 7 - QN. G vs Current.

The major discrepancy between the prediction and measurement was at the highest energisation, where the measured iron-loss was about 1% less than expected. Possible reasons for this are that the BH-curve used in TOSCA was slightly pessimistic, and that a packing factor of 95% was assumed instead of the 98% achieved in practice. These are very important parameters if accurate results are required for a magnet which is operating in a significantly saturated mode.

The results otherwise show agreement with TOSCA to about 1 part in 1000 in gradient distribution, and if the remainder of the QN's are of the same quality as those first delivered, the task of trimming the fields with washers will be trivial.

QFW

Some uncertainty was felt about the outcome of the QFW measurements, principally because of the size of the sextupole component. The results from the first magnet delivered, however, proved to be very satisfactory.

In the centre of the magnet, it was only possible to measure  $\Delta g/g$  within the range  $-12.5 < x < 12.5$  cm, and here the agreement with TOSCA was very good (see Fig. 8). Measurement of  $\Delta G/G$  over the full aperture (Fig. 9) showed differences of up to 1% for large  $|x|$ , which are probably mostly due to the pessimistic BH-curve and packing factor assumed (again 95% as opposed to 98% achieved). However, in the central region the agreement is very good; this justifies the practice of increasing the required sextupole component by  $L_{eff}/L_{iron}$ , for if this had not been done the gradient-integral errors at  $\pm 10$  cm would have been 1%.

In order to meet the field quality specification, the end shims were chamfered to remove most of the excess  $\Delta G/G$  at large  $|x|$ , and the remaining small errors were removed by the use of washers at appropriate locations. Finally, the thickness of the end-shims was trimmed to obtain the correct gradient-integral with the current set to give the required gradient at the magnet centre. The final length over the poles was 0.628 m (0.620 m in TOSCA) and the current  $I = 1782$  A (1823 A in TOSCA).

QDW

Delivery of these magnets is planned for later in 1985, and therefore no measurements have been possible. The results from the QFW, however, give confidence that any field errors will be small and easily corrigible using the shims and washers.

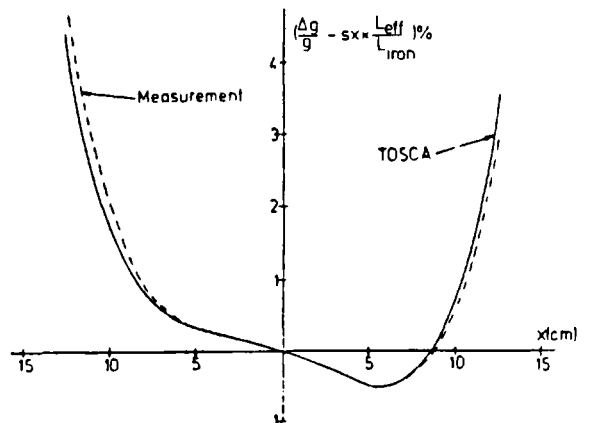


Fig 8 - QFW. g vs x. Prediction and measurement.

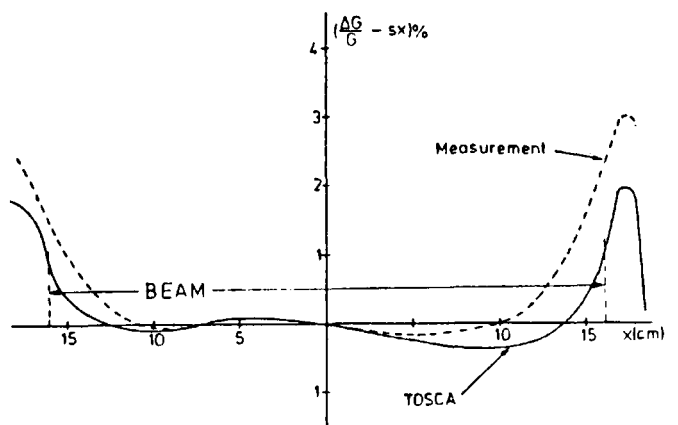


Fig 9 - QFW. G vs x. Prediction and measurement.

## CONCLUSIONS

The decision to rely on computation and to forego prototypes for these magnets has been fully justified by the results. Many man-months of effort, and appreciable time, have been saved by these means; this has been of some considerable importance for a project which has to be completed in as short a time as possible.

TOSCA has been shown to be extremely accurate provided that a) care is taken with the mesh and with the other relevant data, and b) enough computing time is available for its running. With hindsight, the number of computing runs could have been reduced by putting the 6-, 8- and 12-pole terms into the profile all at once.

Finally, it has been shown that extremely large sextupole components can be incorporated into quadrupoles, without the necessity to increase the pole width to maintain linearity: the only limitation is that where the quadrupole and sextupole fields reinforce one another, one should not exceed fields normally asked of a quadrupole.

## APPENDIX

Some technical details concerning the computations are given in Table 2.

TABLE 2

	QN	QW
Number of nodes	15147	20650
Number of conductors (arcs and bars)	5	7
RHS calculation (IBM secs)	1080	1500
Number of iterations (approx.)	30	22
Time per iteration (IBM secs)	280	205
Field calculation per 100 points (IBM secs)	1.7	20.4

## ACKNOWLEDGEMENTS

It is a pleasure to acknowledge the help of the following:

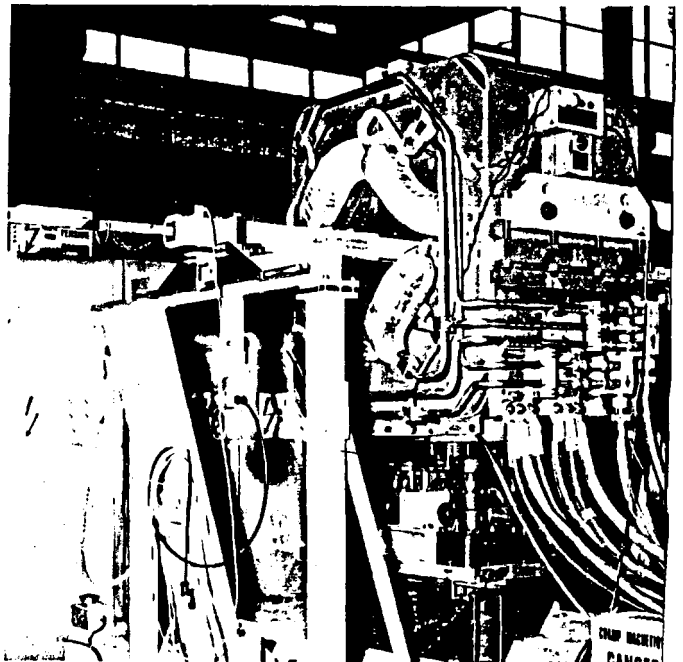
A Armstrong and J Simkin (RAL) set up the QN and QW on TOSCA, and together with C Biddlecombe and C Trowbridge gave much help with the subsequent running of the program.

H Jones (RAL) was responsible for the mechanical design, and B Pincott (CERN) provided an invaluable link with the manufacturers. R Brown resurrected and refurbished the AA apparatus, and together with E Chinchio and G Suberlucq (all at CERN) performed the measurements.

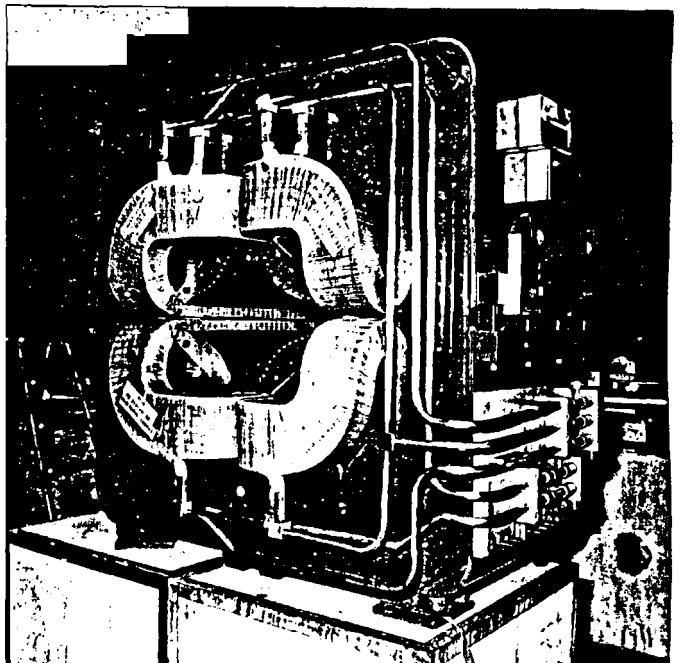
The QN is manufactured by Jeumont-Schneider (France), who also make the coils for the QW's. Tesla Engineering Ltd. (UK) are responsible for the yoke manufacture and assembly of the QW's.

## REFERENCES

- [1] B Autin, The CERN Antiproton Collector, CERN report CERN 84-15.
- [2] B Autin et al., Multipole Fields in the Antiproton Accumulator System, IEEE Trans. on Magnetics, Vol MAG-17, No. 5, p 1591, 1981.
- [3] A Armstrong et al., TOSCA User Guide, Rutherford Lab. Report RL-81-070, 1982.
- [4] C Iselin, CERN Program Library, Long Writeup T600 'MAGNET'.
- [5] C S Biddlecombe et al., PE2D User Guide, Rutherford Lab. Report RL-81-089, 1983.
- [6] M R Harold, Magnet Systems, CERN Accelerator School 1984, Orsay, France (to be published).
- [7] R Brown et al., An Automated Measuring System for the Antiproton Accumulator Magnets, IEEE Trans. on Magnetics, Vol MAG-17, No. 5, p 1864, 1981.



Quadrupole QN



Quadrupole QW